ACS Macro Letters

Letter

pubs.acs.org/macroletters

Mechanotunable Microstructures of Carbon Nanotube Networks

Chao Wang,[†] Bo Xie,[†] Yilun Liu, and Zhiping Xu*

Computational Energetics Laboratory, Department of Engineering Mechanics and Center for Nano and Micro Mechanics, Tsinghua University, Beijing 100084, China

Supporting Information

ABSTRACT: Cohesive but noncovalent interfaces between carbon nanotubes lead to remarkably microstructural evolution of networked materials under mechanical loads. We explore self-organization of these nanofibers, their mechanical properties, and also energy dissipation capacity in response to cycling strain loading. By performing coarse-grained molecular dynamics simulations, the underlying mechanisms are discussed. Their dependence on the strain amplitude and properties of carbon nanotubes are revealed, which opens new possibilities in mechanical tuning of microstructures in carbon nanotubes networks for mechanical, electrochemical, and filtration applications, where the performance is critically defined by microstructures.

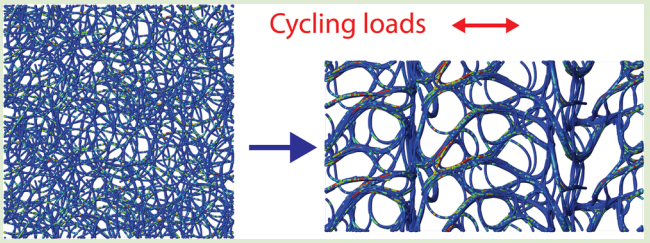

Nanostructured networks of fibrous macromolecules hold great promises in wide applications from multifunctional composites, electrochemical energy storage, to particulate filters, where both pore structures and surface properties are of critical importance to their performance.[1−3] Thus, materials with tunable microstructures are highly demanded, which is usually manifested through energy costly top-down approaches such as templated growth, or alternatively, bottom-up assembly and organization. The latter approach is widely adopted in nature that encodes information from elementary building blocks, interfaces, and environmental cues into the final materials architecture at large scale. This design principle introduces structural hierarchy that fits multifunctional requirements and saves energy inputs.

Low-dimensional carbon nanostructures, such as carbon nanotubes and graphene, are excellent candidates in multifunctional materials according to their outstanding mechanical and transport properties along the extensive directions and simultaneously allowable flexibility (bending, twisting, etc.) in other dimensions. Carbon nanotubes can sustain up to 20% elastic strain before fracture nucleates and are able to be bent reversibly toward an extremely small radius of curvature in a few nanometers. This flexibility can even be further improved through forming localized buckling or rippling structures.[4] In addition to these outstanding mechanical properties, unique thermal, electrical, and electrochemical properties of carbon nanostructures are also attractive for multifunctional applications.[5] A striking example is that ultrathin buckypapers are electrically conducting, 250 times stronger than steel, while 10 times lighter. A recent study shows temperature-invariant viscoelasticity from −196 to 1000 °C, in stark contrast to silicone rubbers that possess much narrower operating temperature window from −55 to 300 °C.[1] Carbon nanotube networks and buckypapers usually feature a porous structure with aggregated single or multiwalled carbon nanotubes by intertube interactions.[6−9] Mechanical properties of carbon nanotube networks and their transport mechanisms are thus determined by networked load-bearing substructures. Rational design on the microstructure of carbon nanotube networks could be optimized to yield high-performance paper materials. To this end, in-depth insights on the relationship between the microstructures and the mechanical properties of carbon nanotubes are needed.

Like other networked materials including rubbers and cytoskeletons, both properties of building blocks and their interactions (cross-links, entanglements, etc.) strongly affect their macroscopic properties.[10−14] Moreover, these microstructures usually evolve under mechanical loading, which further modify material properties. However, this dynamical correlation between the structure and the properties has not been well addressed, whereas a synergetic study combining the power of molecular simulations and fine-scale microscopy observations is required.

In this work, we perform coarse-grained molecular dynamics (MD) simulations to explore the multiscale mechanics of carbon nanotube networks that are shown to be consistent with and offer complement to experimental evidence reported recently.[1,5] In the coarse-grained model for the carbon nanotubes, chains consisting of discrete beads interacting through bond and angle springs (Figure 1) provide a description of tension, bending, and intertube deformation within the continuum mechanics model. The parameters are fit into full-atom molecular dynamics simulations of carbon nanotubes. Each chain consists of 100 beads, as a 100 nm long carbon nanotube. The equilibrium density of the network

Received: August 16, 2012
Accepted: September 17, 2012
Published: September 19, 2012

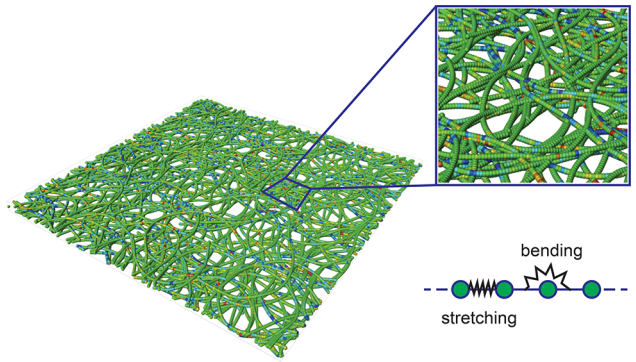

Figure 1. Microstructures of carbon nanotube networks. In the coarse-grained model, stretching and bending terms between the beads correspond to the Young's modulus and bending stiffness of carbon nanotubes, with additional intertube van der Waals interactions.

at the ambient condition is 0.28 g/cm^3. More details about the method can be found in the Supporting Information.

Typical microstructures of carbon nanotubes prepared by simulated deposition are shown in Figure 1, corresponding to a minima in the basin of potential energy surface.[15] The network shows porous structures with diameters up to six nanometers. Bundles form across the whole network where several nanotubes bind locally in parallel, as driven by intertube van der Waals interactions. MD simulations under mechanical loading reported below start from these relaxed load-free structures (see Supporting Information for details).

The mechanical behavior of carbon nanotube networks under monotonic tensile loading was explored by this approach and remarkable microstructural evolution is observed.[15] Under uniaxial tensile loads, alignment along loading direction and bundling are driven by tensile load transfer by extrusion and Poisson's effect in the perpendicular direction. During the loading process, the structure reaches a set of metastable states, which is hinged by local contacts between carbon nanotubes. By tuning chemical cross-links between carbon nanotubes, using noncovalent or covalent bonds, microstructural evolution of the network could be switched on or off.

Our results show the microstructure of carbon nanotube networks changes when cycling loads are applied and converges soon after a few cycles. Figure 2 show microstructures of carbon nanotube networks after 10 loading cycles with peak strain at values ε_p = 0.01, 0.4, 0.8, and 1.2. Corresponding strain-force relations are summarized in Figure 3. Force is used here instead of stress to quantify the resistance to external strain loads. The transverse direction of supercell shrinks remarkably as the tensile load is applied, which leads to drastic enhancement of the stress, while the tensile force offers a more direct measurement for the load bearing and transfer capability than the stress. We observe load-dependent topological changes of, most notably the load-free supercell size and networked structures, i.e. inelastic deformation resulting from structural evolution including nanotube aligning and bundling processes. When the strain amplitude is low (ε_p = 0.01, Figure 3a,d), the network topology is less perturbed when the first-cycle strain load is released except for limited residual compressed stress. The force-strain curves converge soon after the first cycle. Initial response is attributed to local contacts between carbon nanotubes mainly. During further tension, the network is softened with decreasing tangent modulus due to the initiation of alignment, intertube sliding and nonaffine bending deformation. The hysteretic behavior is consistent with recent experimental observations that is responsible to explain the temperature-invariant viscoelastic performance.[1] At the same strain during tensile and compressive loading processes (stages 1 and 2), the local stress states of the networks are not same, which leads to different behaviors in mechanical response and energy dissipation. With our previous understanding on its mechanical behavior under monotonic tensile loading, sliding between carbon nanotubes that induces alignment and bundling occurring at high strain values cannot be significantly activated here. As a result, the microstructure of the network does not show significant changes.

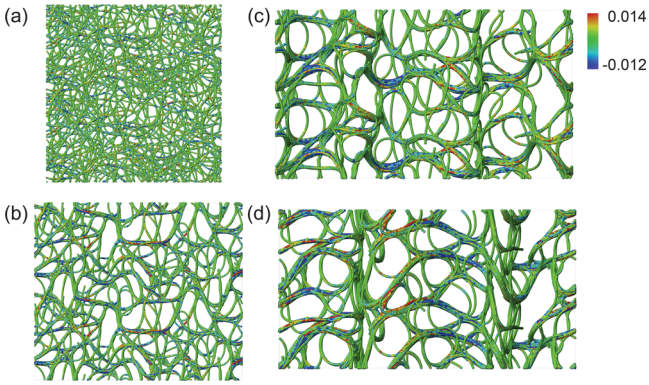

Figure 2. Microstructures of carbon nanotube networks evolved after 10 cycles of strain with peak values at 0.01, 0.4, 0.8, and 1.2. The color represents the local tensile strain in the carbon nanotubes, as indicated in the color bar.

This microstructural pattern is modified substantially as the strain loads increase over a critical value where shear resistance between carbon nanotubes in contact cannot afford the load transferred through this interface. The dominance of elastic deformation to resist external loads is substituted by sliding between neighboring nanotubes, which leads to reduction of contact between nanotubes and significant topological changes. As a result, at intermediate strain, the network sustains notable intertube sliding with alignment of carbon nanotubes to the loading direction and thickening of bundles formed during the loading cycles. At ε_p = 0.4 (Figure 3b,e), during the first tensile cycle, because the strong sp^2 bonds inside the carbon nanotubes bear the load, the contacts between carbon nanotubes are the weakest points in the whole material and fail by exhibiting interfacial sliding. As a result, carbon nanotubes orient in parallel to the loading direction and bear the tensile stress. The whole network self-organizes to maximize contact area and cohesive energy during this process by forming bundles. Upon unloading, the network first sustains a fast elastic unloading (stage 2 as shown in Figure 3b) due to the compressive deformation of nanotubes and bundles well aligned with the loading direction. Then intertube sliding, nanotube reorientation, and limited bundle buckling start to occur, leading to a plateau in force curve as shown in stage 3 in Figure 3b. Similar to ε_p = 0.01, residual compressive stresses remain here after the first cycle. When the second cycle of tensile loading is applied, the network quickly reaches the same maximal stress state as the first cycle, and exhibits similar softening features in stage 1 as ε_p = 0.01. In the third and following cycles, mechanical behaviors of carbon nanotube networks converge as no substantial change of the network structures occur afterward.

dx.doi.org/10.1021/mz300422f | ACS Macro Lett. 2012, 1, 1176−1179

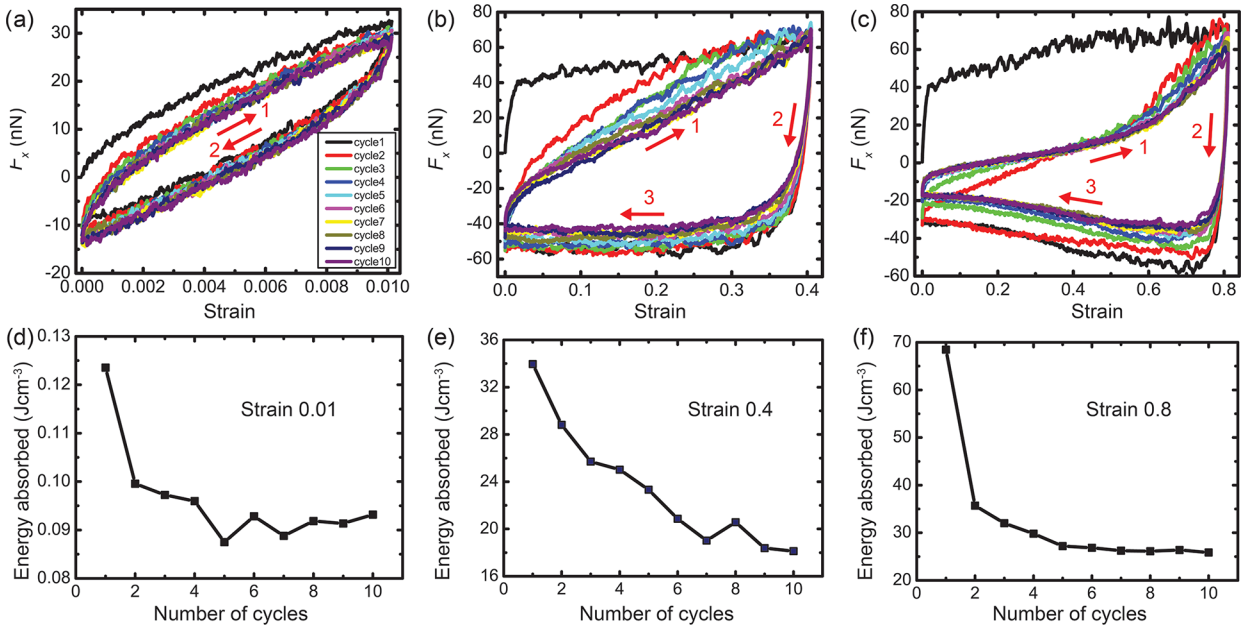

Figure 3. (a–c) Force–strain relationships of carbon nanotube networks under cycling strain loads at 0.01, 0.4, and 0.8. Strain is defined by referring to the original dimension of materials before loading to show the evolution of irreversible deformation. (d–f) Potential energy dissipated through topological changes of the networks, as a function of the number of loading cycles. Numbers 1–3 denotes different loading and unloading stages as mentioned in the text.

At higher deformation amplitudes, the microstructural evolution appears similarly as ε_p = 0.8 (Figures 2c,d and 3c,f). From the second loading cycle, distinct stiffening behavior is observed in stage 1; before that, the mechanical response is attributed to straightening of bent bundles. At higher strain loads than 0.6, sliding at intertube contacts is initialized, yielding higher values of modulus. These responses are different from low and intermediate strain loads where no significant buckling and bending of thick bundles occur. During the first tensile process, the topology of network changes remarkably. Notable nanotube alignment and thick bundling are observed. Bundles align in parallel to the direction of the external load and sustain tensile loads. During the unloading process in stage 2, the stress is released elastically by the rapid compressive response of bundles. Potential energy stored therein is then slowly released by in-plane and out-of-plane buckling of thick bundles to more perpendicular to the load direction in stage 3, which corresponds to the increase of force upon compression or a negative nominal stiffness.

Within each loading cycle, energy stored in the network is dissipated continuously as defined by integrating the force-displacement curve. The energy absorbed is plotted in Figure 3d–f in the unit of J·cm^{-3}, which shows distinct increasing trend with strain amplitudes from the order of 0.1 to 60 J·cm^{-3}, mainly attributed to the formation of thicker bundles. These observations are consistent with recent experimental reports.[1,16] The energy absorption or dissipation capacity is expected to be improved by using multiwalled carbon nanotubes with higher bending stiffness, or better aligned structures.

Porous structures in the carbon nanotube networks are critically important for numerous applications in electrochemical storage, separation, and filtration. The distribution of pore size is clearly tunable by applying cycling strain loads. As shown in Figure 4, networks with larger pore size are formed at higher strain amplitude.

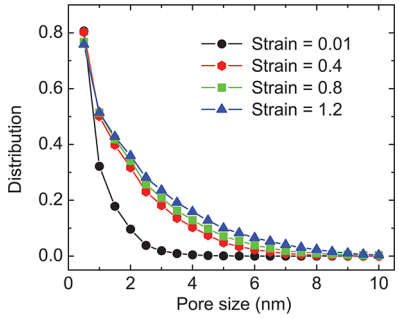

Figure 4. Pore size distribution in carbon nanotube networks at different maximum strain loading amplitudes.

The key mechanism of the strain tuning of network structure is attributed to the noncovalent interface between carbon nanotubes, where large-distance sliding is allowed as assisted by bending deformation of carbon nanotubes. Thus, either by introducing various cross-links at the interface or specific carbon nanotubes with different lengths and diameters could significantly tune the deformation affinity. The effects of cross-links are highlighted in cytoskeleton networks where molecular motors dynamically control the mechanical properties and their biological functions. By using covalent cross-links the well-defined porous microstructures could be "quenched" after specific strain loading is completed. Moreover, by chemically modifying the surface of carbon nanotubes, their interaction could be engineered. Our simulation results in Figure5a show that by enhancing the original interfacial cohesion energy γ_0 = 2.31×10^{-10} J/m, carbon nanotubes align to form thick bundles and strong adhesion between nanotubes could resist higher tensile loads. While as the strength of van der Waals cohesion is reduced, forming contacts and bundles are favored energetically than bending carbon nanotubes. As a result, carbon nanotubes keep straight, topological changes are prohibited, and much lower loads can be transferred.

dx.doi.org/10.1021/mz300422f | *ACS Macro Lett.* 2012, 1, 1176–1179

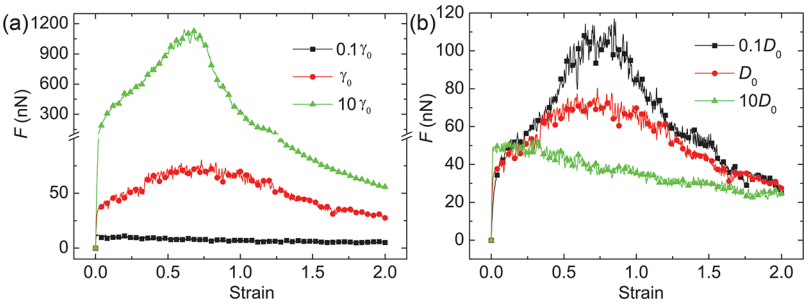

Figure 5. Modified mechanical responses of carbon nanotube networks upon monotonic tensile loading by tuning (a) interfacial cohesion energy γ and (b) bending stiffness D.

The diameter d also controls the persistence length of a carbon nanotube, that is, $l_p = D/k_BT$, where $D_0 = \pi Yd^4/64 = 6.65 \times 10^{-26}$ Nm^2 is the bending stiffness of the carbon nanotube under investigation. Thus, for either multiwalled carbon nanotubes with large diameters or short carbon nanotubes ($l < l_p$), bending deformation and bundling in networks will be limited, and topological changes will be reduced. This is evidenced in our MD simulations where D is magnified by a factor of 0.1 and 10, respectively. As shown in Figure 5b, the resistance to external force is reduced (responses to cycling loads are shown in Figures S1 and S2 in the Supporting Information).

In conclusion, coarse-grained molecular dynamics simulations are applied to explore the responses of carbon nanotube networks under cycling loads. We observe distinct changes in the force-strain relation with strain amplitudes ranging from 0.01 to 1.2. Microstructural evolution and its correlation with mechanical behaviors are discussed, based on which a mechanical tuning strategy of network structures is proposed, with possible controls from loading amplitude, interfacial cross-links and carbon nanotubes. These results offer possibilities to engineer structural and transport properties of nanostructured materials at the network level, with promising applications in electrochemical energy storage, filtration, and separation. The approach we utilize here could also be further extended to include effects from the environment, such as polymer matrices and fluid environment.

■ ASSOCIATED CONTENT

Supporting Information

Detailed description of methods and data for additional cycling loading tests supplementary to the text. This material is available free of charge via the Internet at http://pubs.acs.org.

■ AUTHOR INFORMATION

Corresponding Author

*E-mail: xuzp@tsinghua.edu.cn.

Author Contributions

†These authors contributed equally to this work.

Notes

The authors declare no competing financial interest.

■ ACKNOWLEDGMENTS

This work is supported by the National Natural Science Foundation of China through Young Scholar Grant 11002079, the Tsinghua University Initiative Scientific Research Program 2011Z02174, and Tsinghua National Laboratory for Information Science and Technology, China.

■ REFERENCES

(1) Xu, M.; Futaba, D. N.; Yamada, T.; Yumura, M.; Hata, K. *Science* **2010**, *330*, 1364−1368.
(2) Nyholm, L.; Nyström, G.; Mihranyan, A.; Strømme, M. *Adv. Mater.* **2011**, *23*, 3751−3769.
(3) Halonen, N.; Rautio, A.; Leino, A.-R.; Kyllönen, T.; Tóth, G.; Lappalainen, J.; Kordás, K.; Huuhtanen, M.; Keiski, R. L.; Sápi, A.; Szabó, M.; Kukovecz, A.; Kónya, Z.; Kiricsi, I.; Ajayan, P. M.; Vajtai, R. *ACS Nano* **2010**, *4*, 2003−2008.
(4) Liu, J. Z.; Zheng, Q.; Jiang, Q. *Phys. Rev. Lett.* **2001**, *86*, 4843.
(5) Hahm, M. G.; Wang, H.; Jung, H. Y.; Hong, S.; Lee, S.-G.; Kim, S.-R.; Upmanyu, M.; Jung, Y. J. *Nanoscale* **2012**, *4*, 3584−3590.
(6) Hall, L. J.; Coluci, V. R.; Galvão, D. S.; Kozlov, M. E.; Zhang, M.; Dantas, S. O.; Baughman, R. H. *Science* **2008**, *320*, 504−507.
(7) Gambardella, P.; Dallmeyer, A.; Maiti, K.; Malagoli, M. C.; Eberhardt, W.; Kern, K.; Carbone, C. *Nature* **2002**, *416*, 301−304.
(8) Cooper, S. M.; Chuang, H. F.; Cinke, M.; Cruden, B. A.; Meyyappan, M. *Nano Lett.* **2003**, *3*, 189−192.
(9) Kim, Y.; Torrens, O. N.; Kikkawa, J. M.; Abou-Hamad, E.; Goze-Bac, C.; Luzzi, D. E. *Chem. Mater.* **2007**, *19*, 2982−2986.
(10) Deng, F.; Ito, M.; Noguchi, T.; Wang, L.; Ueki, H.; Niihara, K.; Kim, Y. A.; Endo, M.; Zheng, Q.-S. *ACS Nano* **2011**, *5*, 3858−3866.
(11) Deng, L.; Trepat, X.; Butler, J. P.; Millet, E.; Morgan, K. G.; Weitz, D. A.; Fredberg, J. J. *Nat. Mater.* **2006**, *5*, 636−640.
(12) Kasza, K. E.; Rowat, A. C.; Liu, J.; Angelini, T. E.; Brangwynne, C. P.; Koenderink, G. H.; Weitz, D. A. *Curr. Opin. Cell Biol.* **2007**, *19*, 101−107.
(13) Volkov, A. N.; Zhigilei, L. V. *ACS Nano* **2010**, *4*, 6187−6195.
(14) Cranford, S.; Buehler, M. J. *Nanotechnology* **2010**, *21*, 265706−12.
(15) Xie, B.; Liu, Y.; Ding, Y.; Zheng, Q.; Xu, Z. *Soft Matter* **2011**, *7*, 10039−10047.
(16) Gui, X.; Cao, A.; Wei, J.; Li, H.; Jia, Y.; Li, Z.; Fan, L.; Wang, K.; Zhu, H.; Wu, D. *ACS Nano* **2010**, *4*, 2320−2326.